HEAT AND MASS TRANSFER IN TWO-PHASE HE I THERMOSIPHON FLOW

B. Baudouy

CEA/Saclay, DSM/DAPNIA/STCM
91191 Gif-sur-Yvette Cedex, France

ABSTRACT

Experimental results on two-phase He I natural convection flow, *i.e.* thermosiphon open flow, for a vertical copper tube (14 mm inner diameter) uniformly heated over a length of 1.2 m are presented. Maximum total mass flow rate of 22 g/s and exiting vapor quality factor of 0.2 have been achieved in the steady state regime for a heat flux up to 2000 W/m^2 near atmospheric pressure. In addition, wall temperature difference are measured and critical heat flux and heat transfer coefficients are presented as a function of heat flux. In the nucleate boiling regime, heat transfer coefficient correlations, based on the Martinelli parameter, are proposed for different tube height. They described the data within 20% error margin in the range of 2 10^5 Reynolds number.

INTRODUCTION

The study of heat and mass transfer in a two-phase He I thermosiphon is a part of the design of the cryogenic cooling system of the 4 tesla superconducting solenoid magnet for the Compact Muon Solenoid detector for the LHC under construction at CERN. To maintain the magnet around liquid helium temperature, designers planned to cool this magnet down with a two-phase natural circulation loop [1]. It is in this framework that flow and heat transfer properties in steady state regime are studied in this work. This experimental study aims to measure the different parameters such as the total mass flow rate, the vapor mass flow rate and temperature differences, and determinate heat transfer coefficients and void fraction as a function of the heat flux deposited in the system. Most existing studies on helium boiling vertical two-phase flow are in forced flow configurations [2-7] and only a few experimental works are available, to the best of our knowledge, in the literature concerning natural boiling flow. One on square cross-section tubes having hydraulic diameters around 8 mm with aspect ratio comprised between 110 and 10 [8], the other presents results in an experimental loop to study a two-phase venturi mass flow meter with a 6.35 mm diameter copper tube [9].

EXPERIMENTAL SET-UP

The facility consists of a vertically oriented 2 m long cryostat with vacuum spaces and liquid nitrogen shields. As it is shown in Figure 1, the experimental apparatus is composed mainly of a reservoir that is used as a liquid-vapor separator, a test section and its associated downward tube. The phase separator is 0.3 m high and has a diameter of 0.45 m. The downward tube has a diameter of 40 mm. The test section is made of a 1.2 m Cua1copper tube with 14 mm inner diameter and 1 mm wall thickness. The test section and the separator are completely covered by an aluminum shield cooled by helium vapor flowing out of the separator during the test. The measured static heat load on the experiment is in the order of 0.8 W. The instrumentation consists of two heaters and temperature and pressure sensors. The heaters are soft soldered onto the cooper tube with a twist pitch of 10 mm to create homogeneous heat dissipation. Their resistance is approximately 20 Ω at 4.2 K. Three germanium sensors are inserted in small copper block brazed to the tube and placed along its length. These sensors have been calibrated within 5 mK. The temperature measured here represents that of the inner wall. All wiring is attached to a temperature sink held at 4.2K. There are two mass flow-meters used in this experiment, "a gas flow-meter" at room temperature measuring the vapor mass flow rate and "a Venturi flow-meter" measuring the liquid mass flow rate (*i.e.* total mass flow rate) inside the downward tube. The gas flow-meter is capable of measuring up to 4.2 g/s of He gas at room temperature with a precision of ± 0.01 g/s. The liquid mass flow-meter is a 0.4 m long Venturi with an entry inner diameter of 40 mm and a neck diameter of 10 mm. It is equipped with DP10 Validyne pressure sensor (maximum range of 0.87 kPa), calibrated at 4.2 K within ± 4 Pa. The precision on our mass flow rate measurement varies from 10% for low mass flow rates down to 2% for high mass flow rates. At a high mass flow rate (~20 g/s) the pressure drop within the Venturi constitutes 2% of the total pressure drop.

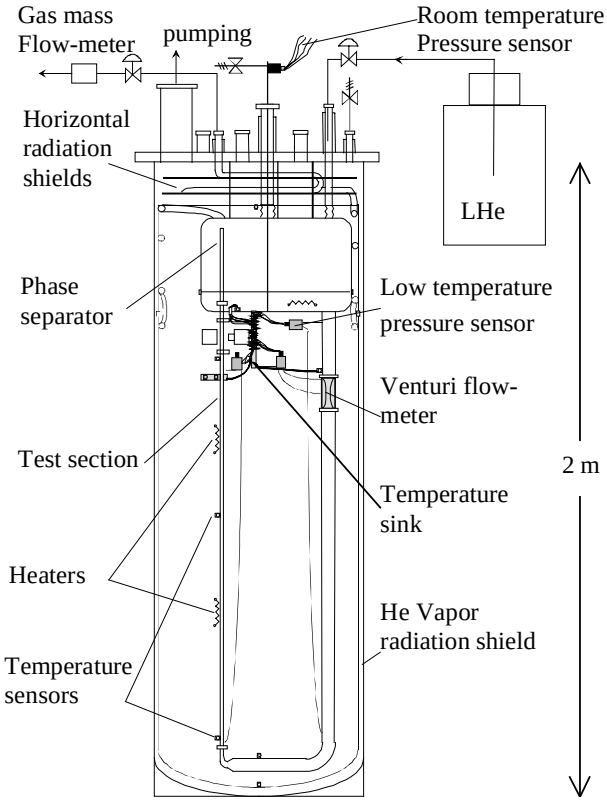

FIGURE 1. Schematic of the experimental set-up.

EXPERIMENTAL RESULTS

Total mass flow rate

Figure 2 presents the evolution of the total mass flow rate, *m*, as a function of heat flux, *q*, over the whole tube length. Different symbols correspond to separate sessions conducted, each with an initial pressure of 990±10 kPa for the entire range of heat flux. Note that the reproducibility is approximately 20% in the low heat flux range, whereas in the higher heat flux range, it reduces to 10%, corresponding to the experimental error. The null shift of the pressure sensor was determined to be around 5 %, giving a partial explanation to our results. For clarity, error bars are shown only for high heat flux range. One finds here the evolution of mass flow rate similar to that of some other types of two-phase mixtures as reported by Jeng *et al.* [10]. A generalized interpretation of the evolution of the mass flow rate in a two-phase mixture is as follows. In the low heat flux region, the gravitational pressure gradient dominates the total gradient in the heated section. As the heat flux increases so as the void fraction, thus, the gravitational pressure gradient would decrease and consequently, a rise in the mass flow rate is induced. In the high heat flux region, it is the frictional pressure gradient that dominates and this continues to grow with increasing void fraction. Then, the mass flow rate diminishes with the increase in the heat flux. Therefore between these two regions, one should observe an intermediate heat flux region where a maximum mass flow rate is achieved. Our results do not exhibit clearly if a maximum mass flow rate has been attained or not. In order to explore the existence of such maximum, we compare our results to other related works. Studies by Huang *et al.* show that the total mass flow rate undergoes a small decrease after attaining a maximum quality factor of 0.2 at the exit of the loop [9]. Here, a maximum quality factor of 0.2 has been obtained at the loop exit ($q \approx 2000$ W/m^2). On the contrary, Johannes *et al.* have demonstrated that a clear maximum is obtained only for a small cross-section (4×0,1 cm^2) [8]. This diminution is short and followed by a brutal upsurge associated with a change in the flow regime. Clearly, further experimental investigations at higher quality factor is needed to characterize the decrease of the total mass flow rate at higher heat flux region.

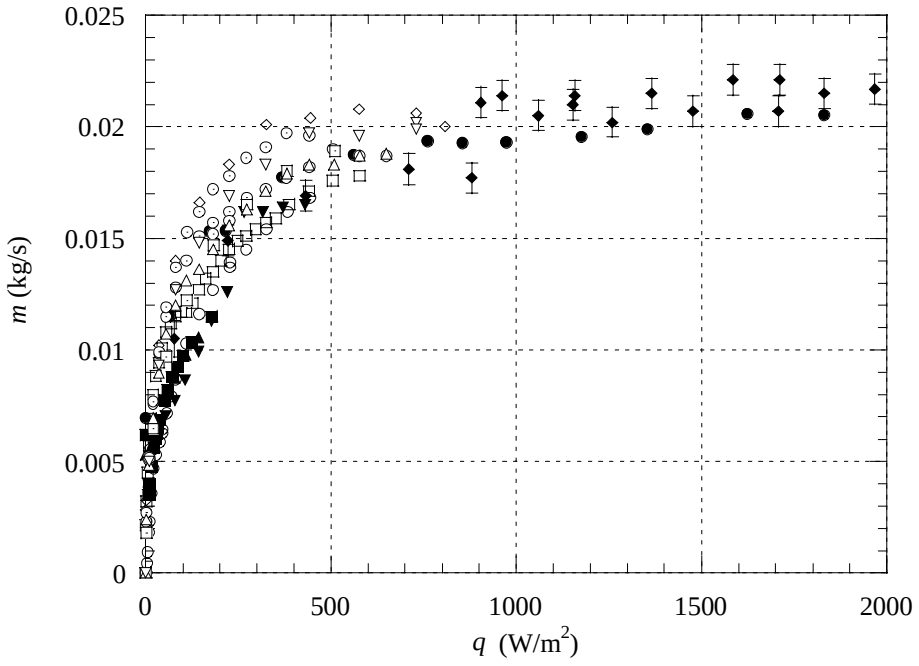

FIGURE 2. Total mass flow rate as a function of the heat flux density.

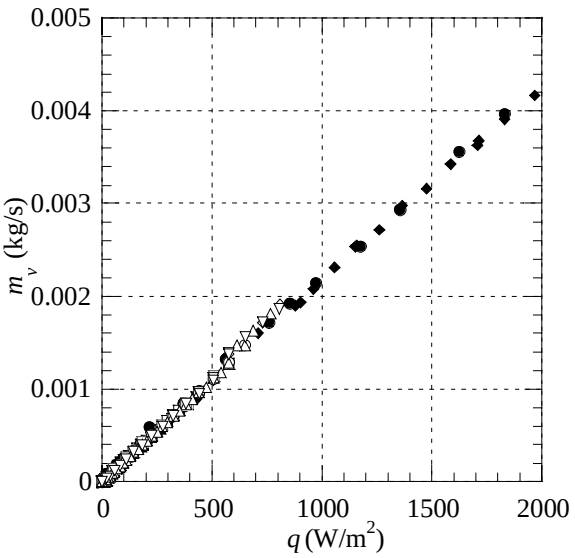

FIGURE 3. Vapor mass flow rate at the exit as a function of heat flux.

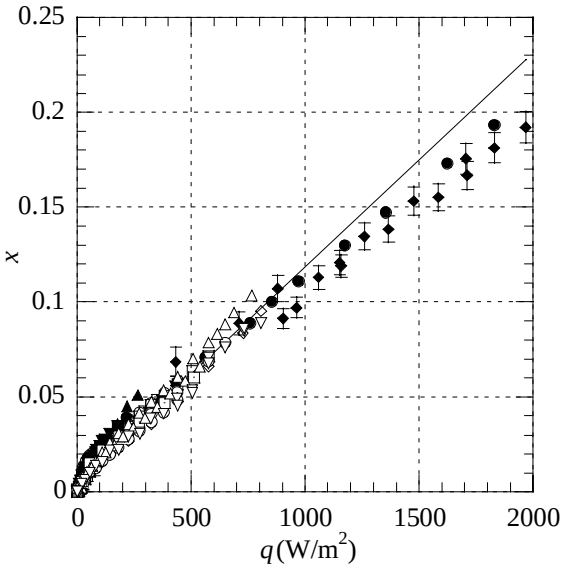

FIGURE 4. Vapor quality at the exit as a function of heat flux.

Vapor mass flow rate and quality factor at the exit

Vapor mass flow rate is measured at the exit of the cryostat at room temperature. Figure 3 presents the evolution of the vapor mass flow rate with the heat flux. Vapor mass flow rate due to the static heat load constituting a systematic error, is subtracted from the experimental data. Note the very good reproducibility of the measurements. From the vapor and total mass flow rates, m_v *and* m, respectively, a quality factor x at the tube exit is determined as $x=m_v/m$. Alternatively, x can be calculated using the heat balance equation taking in account the sub-cooled region for a complete thermodynamic equilibrium [11],

$$x = \frac{\Omega q - mg}{mL_v} H - \frac{C_{p,l}\Delta T_0}{L_v}, \tag{1}$$

where C_{pl} the specific heat of the liquid phase, ΔT_0 the sub-cooling temperature difference, Ω the perimeter of the tube, q the heat flux, L_v the latent heat and H the heated length. This equation is depicted on Figure 4 as a solid line and reproduces with good accuracy the vapor quality evolution up to 1000 W/m^2. The use of this equation is justified if we consider the mixture in thermodynamic equilibrium that seems to be not the case above 1000 W/m^2 as it will be clear in the next section where the temperature difference data are discussed. Partial dry-out appears at the wall in this heat flux range explaining this discrepancy and the origin of non-thermodynamic equilibrium in the flow (Fig. 6 and 7).

Temperature difference at the wall

Fluid temperature, T_f, is measured without applied heat on the test tube. Figure 5 presents the evolution of the temperature difference, ΔT, between the wall, T_w, and the fluid, T_f, as a function of heat flux at 7 cm channel height. If pressure variations are neglected, the heat flux where the sub-cooled zone ends can be calculated from the data by,

$$mC_{pl}\Delta T_0 = \Omega q z_b - mgz_b, \tag{2}$$

where z_b is the sub-cooled height. The heat flux value at the end of the sub-cooled region is between 200 and 300 W/m^2 corresponding to the slope change in Figure 5. One can see

that the evolution of the temperature difference is linear below this heat flux value. In the sub-cooled region, a linear evolution is representative of single-phase convection flow [11]. Sub-cooled boiling can occur in this regime but further analysis is needed to conclude whether there is sub-cooled boiling in our configuration. After the sub-cooled regime, the typical increase in the slope indicates the onset of partial nucleate boiling. This curvature also corresponds to the decrease in the slope of the total mass flow rate as seen in Figure 1 implying the friction loss increase due to the excess in the vapor content. For higher heat flux, $dq/d\Delta T$ becomes more or less constant indicative of the fully developed nucleate boiling [11]. The sub-cooling associated with our experiment is small and around 16 mK which explains the small partial nucleate boiling regime. Figure 5 shows various increases in the wall ΔT all arising from the same heat flux. It has been measured as well as theoretically shown that the existence of multiple values of average velocity in certain heat flux range is a typical aspect of two-phase natural flow [10], [12]. Our results here (also see Fig. 1) confirm such trend. The strong interaction among mass flow rate, heat flux and flow regime in this type of flow creates such a wide spread in the wall ΔT.

Figures 6 and 7 present the ΔT evolution of the flow at different height, namely, 0.6 m and 1.2 m from the tube bottom. These results exhibit drastic jump in ΔT (around 3 to 4 K) that are not shown in Figures 6 and 7. These jumps correspond to local wall dry-out which critical heat flux can be associated. At a height of 0.6 m, the critical heat flux, q_c, is equal to 1400 W/m^2 and at 1.2 m $q_c$is 1200 W/m^2, whereas for a height of 7 cm no critical heat flux has been detected (Fig. 5). In the nucleate boiling regime, the ΔT shows a slight decrease toward the tube exit indicating that the heat transfer coefficient increases with vapor quality (see Fig. 6 and 7). It is a well known fact that the heat transfer coefficient increases with vapor quality [11] and it has been measured in helium and other cryogens in forced flow conditions (See [2] and [7], for example). Nevertheless, for a height of 7 cm, the temperature difference is lower (Fig. 5) and this is also observed by Johannes *et al.* for natural boiling flow [8]. This is probably due to a heat transfer enhancement at the entrance of the tube where the developing flow increases the wall-fluid exchanges.

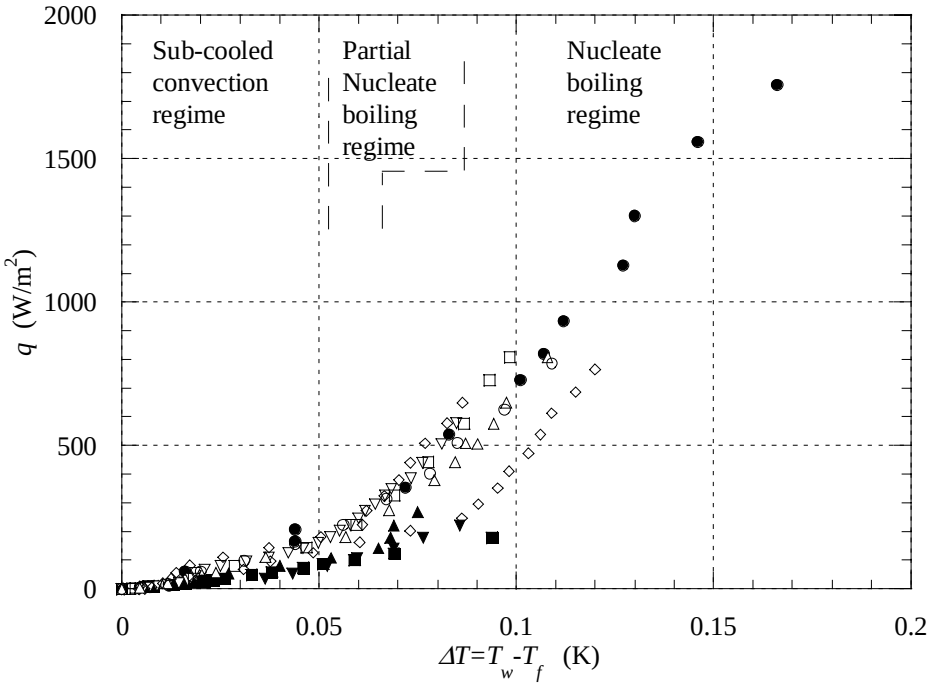

FIGURE 5. Temperature difference as a function of heat flux at 7 cm channel height.

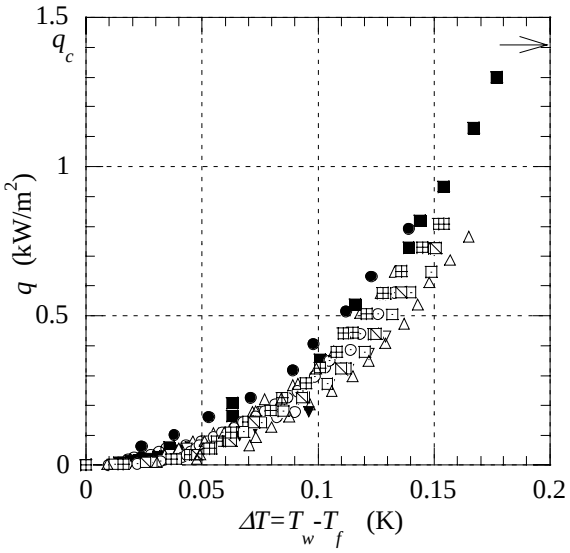

FIGURE 6. Temperature difference as a function of heat flux at 60 cm channel height.

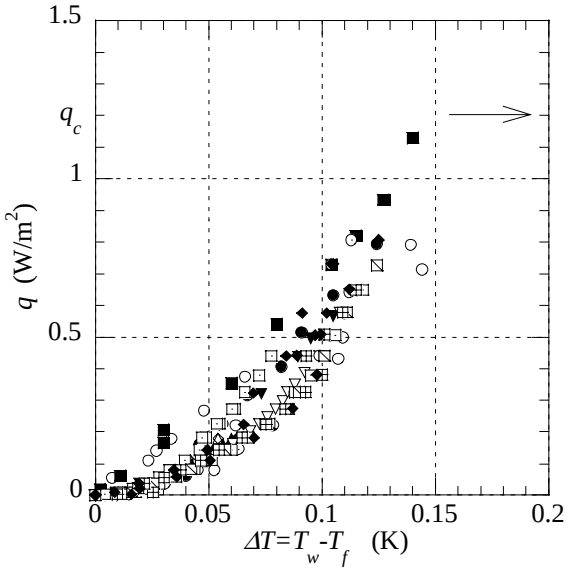

FIGURE 7. Temperature difference as a function of heat flux at 1.2 cm channel height.

Heat transfer coefficient

Heat transfer coefficient, *h*, is determined from wall temperature measurements as,

$$h = \frac{q}{T_w - T_f}, \tag{3}$$

where the temperature of the core mixture is assumed to be the saturation temperature until dry-out. The mixture temperature variation in the sub-cooled regime has been taking in account. Figure 8-a presents the evolution of the heat transfer coefficient as a function of heat flux at a height of 7 cm from the tube bottom. Figure 8-b displays clearly the different regimes: the single-phase convection in the sub-cooled region, the partial nucleate boiling where the heat transfer is almost constant and the fully developed nucleate boiling [11]. In figure 8-a, the heat transfer coefficient for single phase convection, h_l, given by the Dittus-Boelter correlation for turbulent flow is also plotted,

$$h_l = 0{,}023 Re_l^{\,0,8}\, \mathrm{Pr}_l^{\,0,4}\, \frac{d}{k_l}, \tag{4}$$

where Re_l, Pr_l, k_l, d are respectively the Reynolds number, the Prandtl number, the thermal conductivity of the liquid phase and the tube diameter, respectively. The heat transfer coefficient can be as high as 2.5 times the Dittus Boeltler correlation. Numerous heat transfer correlations exist in the literature taking in account the effect of thermally and hydrodynamically developing flow on heat transfer with different configuration such as elbow entrance and heating section. The developing flow effect can enhance the heat transfer coefficient by at most 100%, clearly, not sufficient to explain our previous measurement [13]. We believe that, the enhancement of the heat transfer coefficient is also due to sub-cooled boiling because the wall temperature difference is already above the sub-cooling (16 mK) at 40 W/m^2.

Heat transfer coefficients around 500 W/m^{2}K are found after dry-out at 0.60 m and 1.2 m (see Fig. 9 and 10). These coefficients correspond to film boiling where a vapor film is created and maintained at the wall. The critical heat flux, associated with dry-out, decreases with increasing channel height in agreement with other works [3], [8], [11].

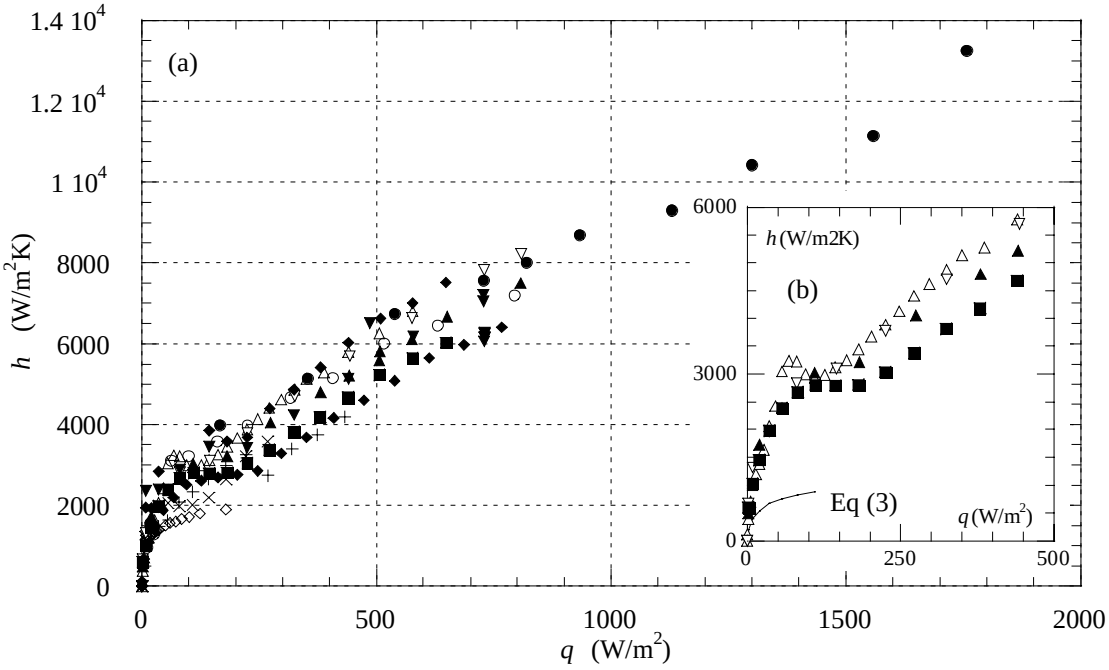

FIGURE 8. Heat transfer coefficient as a function of heat flux at function at 7 cm channel height.

In the fully developed nucleate boiling regime (Fig. 9 and 10), an attempt is made to correlate heat transfer data with the widely used method proposed by Martinelli. It should be noted, that in this model, it is that the wall is assumed to be principally in contact with the liquid phase, *i.e.* in a low vapor quality regime [11]. The correlation is described by

$$h_{TP} = h_l A X_{tt}^{-n} \tag{5}$$

where h_{TP} is the two-phase heat transfer coefficient, h_l the heat transfer coefficient given by the Dittus-Boelter law Eq. (3) and X_{tt} is the Lockhart-Matinelli parameter defined as,

$$X_{tt} = \left(\frac{1-x}{x}\right)^{0.9}\left(\frac{\rho_v}{\rho_l}\right)^{0.5}\left(\frac{\mu_l}{\mu_v}\right)^{0.1} . \tag{6}$$

ρ_l, ρ_v, μ_l, μ_v are the density and viscosity of the liquid and vapor phase respectively. For both channel heights, 0.6 m and 1.2 m, the exponent n is 0.5, whereas the proportional factor *A* is found 12 for 0.6 m height and 9 for 1.2 m height. The correlation presented here describe most of the data within 20% error margin for $10^5 \le Re \le 6\ 10^5$ and $2 \le X_{tt} \le 50$.

Johannes has also applied the same correlation for helium forced flow on Monel tubes with diameters from 2 to 3 mm and a range of heat flux density and X_{tt} identical to our experiment [2]. They found the best fit with A=5.4 and n=0.385. Their correlation underestimates our experimental data by a factor of two. Ogata and Sato performed measurements in turbulent boiling helium forced flow in a 11 mm diameter tube up to Re of $7\ 10^4$. They used a more sophisticated correlation, $h_{TP}/h_l = X_{tt}^{-0.66} + 1500 Bo^{0.8}$, where *Bo* is the boiling number ($Bo = qG/L_v$). This correlation also underestimates our data by a factor of two. Both results seem to indicate that heat transfer coefficients in boiling two-phase open flow are higher than in forced flow for the same reason evoked for the enhancement of *h* in the sub-cooled regime. The difference between forced flow and boiling flow is that boiling flow is always in development thermally and hydrodynamically [10], thus friction factor and heat transfer coefficient are underestimated by forced convection theories. More sophisticated methods for correlating heat transfer data can be used depending on several parameters, such as pressure and sub-cooling, for example, that were not investigated here.

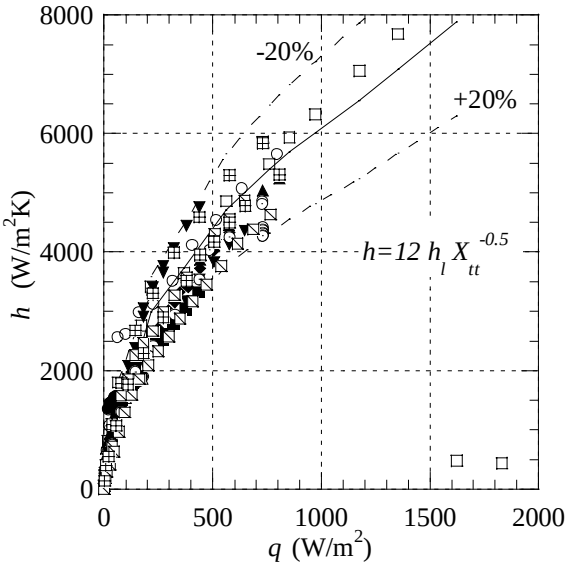

FIGURE 9. Heat transfer coefficient as a function of heat flux as a function at 60 cm channel height.

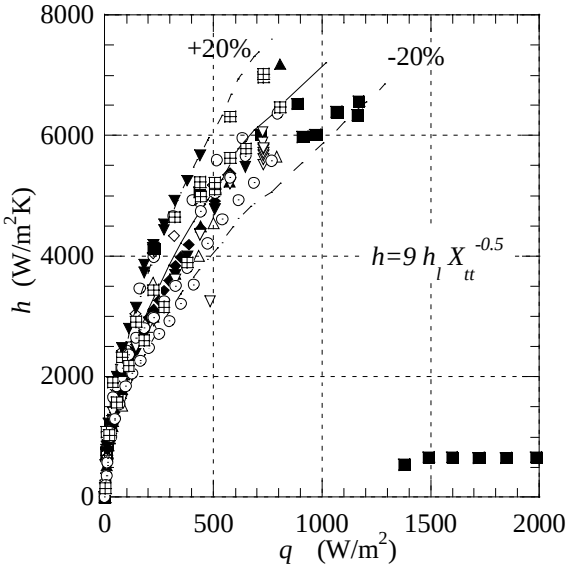

FIGURE 10. Heat transfer coefficient as a function of heat flux as a function at 1.2 m channel height.

CONCLUSIONS

Helium two-phase boiling convection at atmospheric pressure have been performed up to a vapor quality of 0.2 and mass flow rate of 22 g/s. Heat transfer coefficients are higher than in boiling helium forced flow due to developing flow. For small channel height, in the sub-cooled region, boiling seems to enhance also the heat transfer coefficient. In the nucleate boiling region, heat transfer coefficient are correlated by the form $h_{TP} \propto h_l X_{tt}^{-0.5}$ depending on the channel height within 20% error margin for $10^5 \leq Re \leq 6\ 10^5$ and $2 \leq X_{tt} \leq 50$.

ACKNOLEDGEMENTS

The author would like to thank D. Thomas for technical support, Dr. Juster and Dr. Brédy for helpful discussions and Dr. Kircher for financial support.

REFERENCES

1. Lottin, J. C. and Juster, F.-P., "Liquid Helium Thermosiphon For the 4 Tesla CMS Solenoid" in *Adv. Eng. Cryo* 43, edited by P. Kittel, Plenum Press, 1998, pp. 1505-1511.
2. Johannes, C., "Studies of forced convection heat transfer to helium I" in *Adv. Cryo. Eng.* 17, edited by K. Timmerhaus, Plenum Press, 1972, pp. 352-360.
3. Giarrantano, P. J., *et al.*, "Forced convection heat transfer to subcritical helium I" in *Adv. Cryog. Eng.* 19, edited by K. Timmerhaus, Plenum Press, 1974, pp. 404-416.
4. Ogata, H. and Sato, S., *Cryogenics*, **vol. 14**, pp. 375-380, (1974).
5. Keilin, V. E., *et al.*, *Cryogenics*, **vol. 15**, pp. 141-145, (1975).
6. Deev, V. I., *et al.*, *Thermal Engineering*, **vol. 32**, pp. 680-682, (1985).
7. Grigor'ev, V. A., *et al.*, *Thermal-Engineering*, **vol. 24**, pp. 12-15, (1978).
8. Johannes, C. and Mollard, J., "Nucleate boiling of helium I in channels simulating the cooling channels of large superconducting magnets" in *Adv. Cryo. Eng.* 17, edited by K. Timmerhaus, Plenum Press, 1970, pp. 332-341.
9. Huang, X. and Van Sciver, S. W., *Cryogenics*, **vol. 36**, pp. 303-309, (1996).
10. Jeng, H. R. and Pan, C., *Annals of Nuclear Energy*, **vol. 26**, pp. 1227-1251, (1999).
11. Collier, J. G., *Convective boiling and condensation*, McGraw-Hill, London, 1972.
12. Lee, S. Y. and Lee, D. W., *Nuclear Engineering and Design*, **vol. 128**, pp. 317-330, (1991).
13. Kakac, S., *et al.*, *Handbook of single-phase convective heat transfer*, John Wiley & Sons, 1987.